Information Sciences 000 (2018) 1–14

Contents lists available at ScienceDirect

Information Sciences

journal homepage: www.elsevier.com/locate/ins

A hand-based biometric system in visible light for mobile environments

Silvio Barra[a,*], Maria De Marsico[b], Michele Nappi[c], Fabio Narducci[c,*], Daniel Riccio[d]

[a] Dipartimento di Informatica, Università degli Studi di Cagliari, Cagliari, Italy
[b] Dipartimento di Informatica, Sapienza Università di Roma, Roma, Italy
[c] Dipartimento di Informatica, Università degli Studi di Salerno, Fisciano, Salerno, Italy
[d] Dipartimento di Informatica, Università "Federico II" di Napoli, Napoli, Italy

ARTICLE INFO

Article history:
Received 11 August 2017
Revised 4 January 2018
Accepted 7 January 2018
Available online xxx

Keywords:
Hand geometry
Hand recognition
Mobile devices

ABSTRACT

The analysis of the shape and geometry of the human hand has long represented an attractive field of research to address the needs of digital image forensics. Over recent years, it has also turned out to be effective in biometrics, where several innovative research lines are pursued. Given the widespread diffusion of mobile and portable devices, the possibility of checking the owner identity and controlling the access to the device by the hand image looks particularly attractive and less intrusive than other biometric traits. This encourages new research to tacklethe present limitations. The proposed work implements the complete architecture of a mobile hand recognition system, which uses the camera of the mobile device for the acquisition of the hand in visible light spectrum. The segmentation of the hand starts from the detection of the convexities and concavities defined by the fingers, and allows extracting 57 different features from the hand shape. The main contributions of the paper develop along two directions. First, dimensionality reduction methods are investigated, in order to identify subsets of features including only the most discriminating and robust ones. Second, different matching strategies are compared. The proposed method is tested over a dataset of hands from 100 subjects. The best obtained Equal Error Rate is 0.52%. Results demonstrate that discarding features that are more prone to distortions allows lighter processing, but also produces better performance than using the full set of features. This confirms the feasibility of such an approach on mobile devices, and further suggests to adopt it even in more traditional settings.

1. Introduction

In the last fifteen years, the adoption of biometric systems has ranked among the safest security measures to enforce access control, also against attempts of identity theft [10]. This is due to the possibility to automatically discriminate people

* Corresponding authors.
E-mail addresses: silvio.barra@unica.it (S. Barra), demarsico@di.uniroma1.it (M. De Marsico), mnappi@unisa.it (M. Nappi), fnarducci@unisa.it (F. Narducci), daniel.riccio@unina.it (D. Riccio).

https://doi.org/10.1016/j.ins.2018.01.010

basing on their physical or behavioural characteristics. Though their birth can be approximately situated in the last decades of the 1800 [8], the world witnessed their first (r)evolution in the late 90's, when they started replacing some traditional identification system [27]. Since then, the popularity and reliability of biometric systems kept rising. They are presently used to chase high levels of security in different real life applications, from videosurveillance [25,33,34] to smartphone authentication and access control to restricted areas [3,5].

Nowadays the use of mobile devices, and especially of smartphones, has spread like wildfire. As a consequence, many biometric systems Are rapidly migrating to these devices. The embedded dual camera mode offers the possibility to acquire different biometric traits on-the-fly, in order to grant access to the functionalities of the smartphone itself. Up to now, face [6,12], iris [1,5] and ear [4] have been widely explored in the mobile context, even though international challenges (e.g., see [9,13,14]). In all such cases, the acquisition of the biometric sample is based on the shot of an image. Many other traits are historically acquired by different external contact sensors. Palmprints and fingerprints, for example, are well-known traits acquired by ad-hoc sensors. Such sensors are able to capture very tiny minutiae with high precision, in order to obtain a high discriminating power. However, they are quite costly, and the largest ones (i.e., for palmprint) may not be generally easy to embed in mobile devices. Furthermore, since they require direct contact, they are quite intrusive and scarcely hygienic, and require frequent cleaning. These factors pose limitations to the spread of the related technologies in mobile environments. Similarly, the shape of the hand has also been long acquired by specialised 2D or 3D scanners. That specialised hardware has the benefit of providing a good quality acquisition and, according to the conditions and constraints, often produces a strong separation between the foreground (the hand) and the background (which represents useless information). After being investigated in digital image forensics, hand shape has gained popularity in biometrics too. With respect to other biometric traits, e.g., face and fingerprints, much less studies have tackled the feasibility of using hand features alone for biometric recognition. However, even for this trait, the widespread diffusion of mobile and portable devices has spurred new research lines. The possibility of checking the owner of and controlling the access to the device by the hand image looks particularly attractive and less intrusive than other biometric traits, but the use of special hardware must be avoided. This paper presents a solution for hand shape recognition, which is completely built around the embedded RGB camera and the processing power of a mobile device, in particular of a smartphone. The proposed work represents an extension of a previous work [7], that dealt with an initial investigation on the extraction of relevant measures from the hand shape and geometry. The characterizing elements of the proposed approach are the lack of contact with any sensor surface, the lack of (physical) pegs, and the use of a mobile device. Moreover, the matching procedure does not use the complete set of extracted features, as in other works in literature. We investigated different approaches to rather identify a suitable subset of them to attain a twofold goal. In the first place, some of the geometric features, that can be extracted from hand shape, are more prone to distortions caused by, e.g., slightly different distance or relative orientation of the hand and device camera. Results demonstrate that discarding those less robust features, allows achieving better performance than using the full set. As an added value, the resulting lighter matching procedure can be better carried out on mobile devices, which are the main target of this work. The contribution of this work can be identified along these two lines. On one hand, it presents a deeper investigation on different techniques for the analysis of the original feature space. The aim is individuating the most informative and robust features with respect to the recognition performance on a mobile device. On the other hand, it explores further matching approaches, to better understand how the selected subset of features generalises over a representative set of classification techniques.

The paper is organised as follows. Section 2 discusses related works. Section 3 introduces the proposed processing pipeline, and two different analysis approaches to identify the most informative and therefore discriminative features. Section 4 presents and discusses the experimental setup and the achieved results, detailing the exploited dataset, and the methods used for matching. Section 5 summarises the achievements of the proposal and sets lines of future investigation.

2. Related work

Hand-based biometric systems can use a broad set of parameters, computed by processing an acquired hand image. These systems generally either measure and analyse the overall structure, shape and proportions of the hand (e.g., length, width and thickness of hand, fingers and joints), or extract characteristics of the skin surface of the palm, such as furrows and ridges (i.e., the palmprint), or rely on the vein pattern on the back. Earlier methods proposed in literature fall in the first group and require the user to keep the hand in a predefined, fixed position [35,41]. For instance, in [37] an ordinary CCD color camera is placed over a plate. This is equipped with some driving pegs, that guide the user to put the hand in a specific position. Pins are activated by the pressure of the user hand. Once all of them are activated, the camera acquires the biometric trait (hand image) for processing. These techniques benefit from the strictly controlled acquisition. Consequently, measures and characteristics are quite robust for both intra- and inter-user recognition. The reverse of the medal is represented by the controlled settings, and by the need for full collaboration by the users and for special equipment. Moreover, the implementations that have been used for years required the physical contact with the acquisition device (contact-based solutions). This further poses problems related to the personal hygiene and health of the user.

Palmprint is a well-known biometric trait used for full hand recognition [23]. Present palmprint scanners simplify the development of the recognition algorithms, with respect to traditional peg-equipped plates, but also require a suitable selection of lens, camera, and light sources [43]. Most of all, they still work by direct contact. Apart from health issues, the physical contact may lead by itself to distortions of the characteristics of the palmprint, e.g., due to the pressure exerted by

Please cite this article as: S. Barra et al., A hand-based biometric system in visible light for mobile environments, Information Sciences (2018), https://doi.org/10.1016/j.ins.2018.01.010

the user on the glass of the scanner. Moreover, the palmprint scanners cannot be easily moved from one position to another. Last but not least, they can be hardly used in real-time operations due to the scanning time. Therefore, they result in solutions that are completely inappropriate for many applications. These limitation have spurred the search for alternative capture protocols. More recent works have demonstrated that digital video cameras can be effective to collect palmprint images without contact [15,19]. For instance, the system described in [17] uses two commercial cameras (i.e., a RGB camera and an IR camera) placed beside to each other. The illumination is controlled by an external light source (composed of white and infrared leds), which ensures a global illumination of the hand. This must be placed in front of the cameras. The resulting system exploits a score fusion over results from matching hand geometric features and palmprint features, in order to achieve a high recognition accuracy. The work in [2] proposes a method for the segmentation of a hand image from a complex background by a stereo acquisition system including two RGB cameras. On the contrary, the work by Sanches et al. [36] proposes an approach based on a single RGB camera to extract several hand features from the input image. The approach entails a decision level fusion of the results from matching biometric features related to hand geometry, palmprint and finger surface, and reaches a recognition rate above 98%. The possibility of using ordinary RGB cameras for palmprint recognition suggests that these solutions might be feasible for mobile devices too. However, limitations of mobile cameras may negatively affect the recognition performance. For instance, their resolution is generally lower, and this may hinder the acquisition of thin details. In addition, their intended use is to acquire images in uncontrolled settings, with possible illumination variations and distortions also due to the hand movements. In the case of hand sample acquisition, these movements involve both the hand handling the mobile device and the hand being captured. They represent with no doubt the most challenging aspects of contact-less hand recognition, due to the lack of constraints for the user on how and where to place the hand in front of the camera. In fact, the distance from the camera and the appearance of the hand may vary significantly in a sequence of acquisitions by the same subject. In particular, if the hand surface is not perfectly orthogonal (e.g., perpendicular to the camera view axis), the inclination may lead to incorrect measurements of the hand geometry. However, hand geometry processing is less affected by possible poor resolution of mobile cameras than palmprint processing. The contact-less system in [38] is based exclusively on the use of hand shape and geometry. Several other works in the last five years exploit measures extracted from hand geometry for subject recognition; in particular [39] exploits 121 features plus the contour of the hand to achieve an EER (Equal Error Rate) of 0.52%. The authors of [26] propose a method based on genetic algorithms and LDA to reach 4.9% of EER by using 34 features. Other interesting works worth to be cited are [32] (that exploits palm and back of the hand) and [21](that achieves an EER of 3.69% by using the Fourier descriptor and weighted sum score fusion over four hand fingers).

The method proposed here extracts 57 features from the hand shape geometry. The idea has been implemented for mobile devices, and hence the hand features are extracted from images captured in uncontrolled settings. In order to reduce the number of features, by discarding the less informative and robust ones, two different methods of analysis are compared. The first one ranks the features according to the achieved *Decidability* value. The second one ranks them according to the Intra-class to Inter-class variability ratio. The best classification results are achieved by the Linear Discriminant Analysis (LDA).

3. Proposed system

This section first presents the capture procedure and the following processing to extract features from hand images. Then two alternative analysis strategies are proposed, based on different metrics, to identify the most representative as well as robust subset of features to use for matching. The aim of this analysis is twofold. On one side, discarding those features that appear to be more subject to distortions across images of the same hand can improve the overall recognition accuracy. On the other side, using less features for matching allows a lighter processing, that is better suited to be carried out on mobile devices.

3.1. Image capture and feature extraction

The proposed system is built for Android mobile devices. The application is written in Java through the native Android Software Development Kit (SDK) and OpenCV for mobile. The capture module exploits the rear camera to acquire the user hand.

Fig. 1 depicts the few steps making up the user enrolment. The first one is the acquisition of the hand image. The user is asked to put the hand in front of the camera, and to ensure that five reference areas displayed on the screen are filled with the colour of the skin. The aim of these reference areas is twofold. First, they help the user to understand how to properly place the hand in front of the camera, therefore playing a similar role of pegs but in a much less constrained way. In addition, they are also used to extract reference colours to generate five different segmentations of the hand. The acquired RGB frame is first converted into the HSV colour space. The Hue channel is used to filter the image and to produce a distinct segmentation in relation to to each of the five colours extracted from the areas mentioned above. These segmentations are computed according to a corresponding set of thresholds, which are determined as follows. For each reference area, the arithmetic mean m_i $(i = 1, \ldots, 5)$, of the hue values of its pixels is computed. Given the obtained mean m_i, a binary

Please cite this article as: S. Barra et al., A hand-based biometric system in visible light for mobile environments, Information Sciences (2018), https://doi.org/10.1016/j.ins.2018.01.010

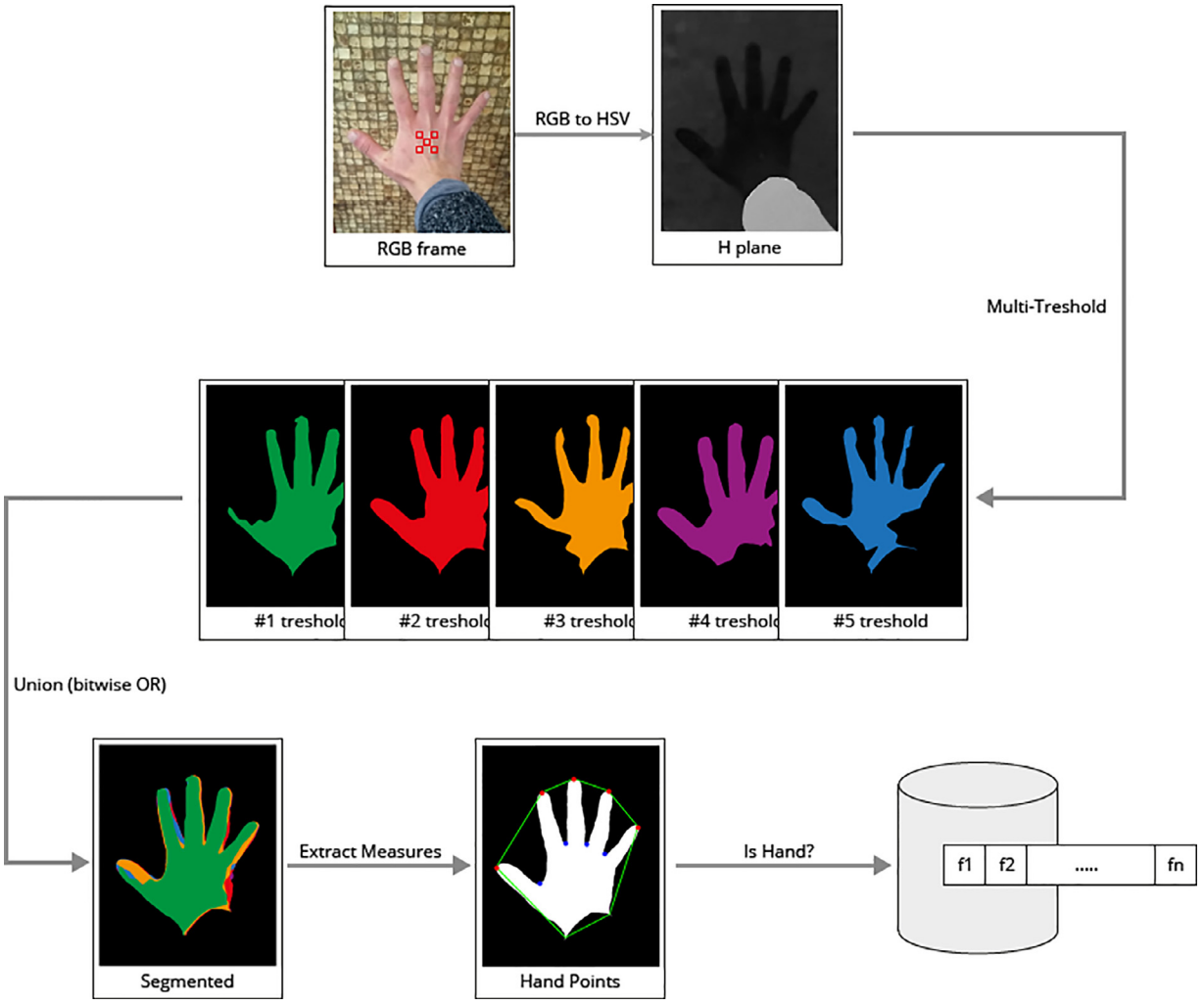

Fig. 1. The overall view of the process of segmentation and feature extraction.

segmentation mask S_i is generated according to the following rule:

$$S_i(p_j) = \begin{cases} 1 & \text{if } m_i - k \leq H(p_j) \leq m_i + k \\ 0 & \text{otherwise} \end{cases} \quad (1)$$

where p_j is a pixel in the original image, $H(p_j)$ is the hue value of that pixel in the original image, and k is a constant that defines the amplitude of the hue range for the skin. According to the results of an empirical study, we set this value to $k = 4$. However, it can be customised according to the camera characteristics in order to improve the quality of the segmentation. The five obtained segmentation masks are post-processed by morphological operators to further improve their accuracy, by removing noise, holes and blobs. Finally, they are combined by a union operation (a bitwise OR), to generate a single final binary mask.

Before using the final segmentation mask to extract relevant geometry measures related to the hand shape, the system first checks if the obtained segmentation can represent a hand. It determines the convexities (represented by points $P1, \ldots, P5$ in Fig. 2) and concavities, or convexity defects (represented by points $V1, \ldots, V4$ in Fig. 2) in the mask to count the number of possible fingers, that should be a complete set of 5. If the control succeeds, the application uses the mentioned points to compute the measures needed for the following matching process.

The measures that are taken into account can be divided into four classes: (1) lengths; (2) ratios; (3) areas; and (4) angles. Fig. 2 shows all the measures that have been computed from the shape of the segmented hand, while Table 1 provides details on these measures, which have been labelled with a code to improve the readability of the results (i.e., f1, f2, f3, ...).

Please cite this article as: S. Barra et al., A hand-based biometric system in visible light for mobile environments, Information Sciences (2018), https://doi.org/10.1016/j.ins.2018.01.010

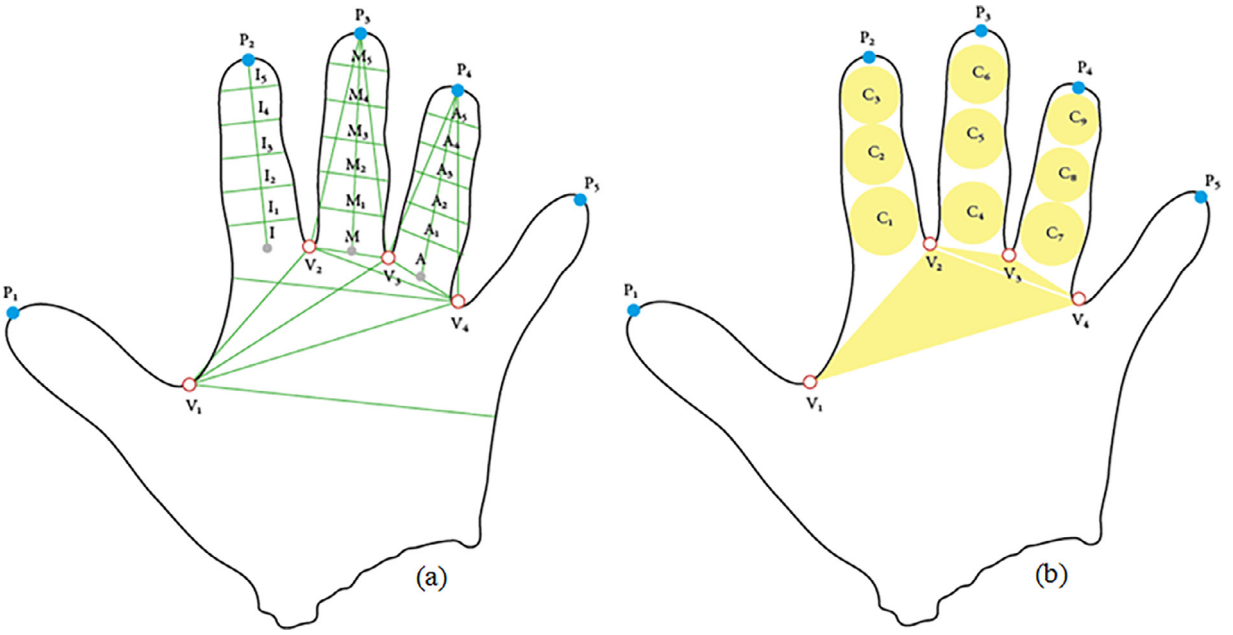

Fig. 2. The measures over the hand shape. (a) The reference points P_i and V_i from which lengths are computed, and further segments determined over the fingers and the palm. (b) Triangular and circular areas extracted from the reference points in (a)

Table 1
List of the measures computed over the segmented hand.

LENGTHS	**f1**: $\overline{V1V2}$	**f2**: $\overline{V1V3}$	**f3**: $\overline{V1V4}$	**f4**: $\overline{V2V3}$
	f5: $\overline{V3V4}$	**f6**: $\overline{V2V4}$	**f7**: $\overline{P_2I}$	**f8**: $width(I_1)$
	f9: $width(I_2)$	**f10**: $width(I_3)$	**f11**: $width(I_4)$	**f12**: $width(I_5)$
	f13: $\overline{P_3M}$	**f14**: $width(M_1)$	**f15**: $width(M_2)$	**f16**: $width(M_3)$
	f17: $width(M_4)$	**f18**: $width(M_5)$	**f37**: f_{19}/f_6	**f20**: $width(A_1)$
	f21: $width(A_2)$	**f22**: $width(A_3)$	**f23**: $width(A_4)$	**f24**: $width(A_5)$
	f25: $\overline{V_2P_3}+\overline{P_3V_3}$	**f26**: $\overline{V_3P_4}+\overline{P_4V_4}$	**f27**: $f_8+\cdots+f_{12}$	**f28**: $f_{14}+\cdots+f_{18}$
	f29: $f_{20}+\cdots+f_{24}$	**f30**: $width(V_1)$		
RATIOS	**f31**: f_1/f_6	**f32**: f_2/f_6	**f33**: f_3/f_6	**f34**: f_6/f_4
	f35: f_7/f_6	**f36**: f_{13}/f_6	**f37**: f_{19}/f_6	**f38**: $(f_7+f_{13}+f_{19})/f_6$
	f39: f_{30}/f_{13}	**f40**: f_{50}/f_{51}		
AREAS	**f41**: A_{C_1}	**f42**: A_{C_2}	**f43**: A_{C_3}	**f44**: A_{C_4}
	f45: A_{C_5}	**f46**: A_{C_6}	**f47**: A_{C_7}	**f48**: A_{C_8}
	f49: A_{C_9}	**f50**: $A_{V_1V_2V_4}$	**f51**: $A_{V_2V_3V_4}$	
ANGLES	**f52**: $\widehat{V_2V_3V_4}$	**f53**: $\widehat{V_3V_4V_2}$	**f54**: $\widehat{V_4V_2V_3}$	**f55**: $\widehat{V_1V_2V_4}$
	f56: $\widehat{V_2V_4V_1}$	**f57**: $\widehat{V_4V_1V_2}$		

3.2. *Feature analysis by* Decidability *measure*

The *Decidability* index is the normalized distance between means of genuine and imposter distributions [40] and is defined as follows:

$$dec = \frac{|avg(D^I) - avg(D^E)|}{\sqrt{(0.5 * (std(D^I)2 + std(D^E)2))}} \tag{2}$$

where $D^I = D^I_1, \ldots, D^I_k$ is the set of intra-subject dissimilarity values (obtained by matching pairs of templates belonging to the same subject) and $D^E = D^E_1, \ldots, D^E_m$ is the set of inter-subject dissimilarity values (obtained by matching pairs of templates belonging to different subjects).

The barplot in Fig. 3 is MIN/MAX normalised in the range [0, 1] and reports the *Decidability* values dec_i achieved by each of the 57 characteristics f_i taken into account. Since this index can be considered as a way of separating reliable features from the poorer ones, such plot can allow visually comparing the reliability of the features. It is possible to apply a thresholding approach to identify a collection of different subsets of the features with the aim of comparing and minimising the EER achieved. In more detail, subsets can be defined according to the following rule:

$$F_j = \left\{ f_i : dec_i \geq \tau_j \right\} \; with \; 0 \leq \tau_j \leq 1 \tag{3}$$

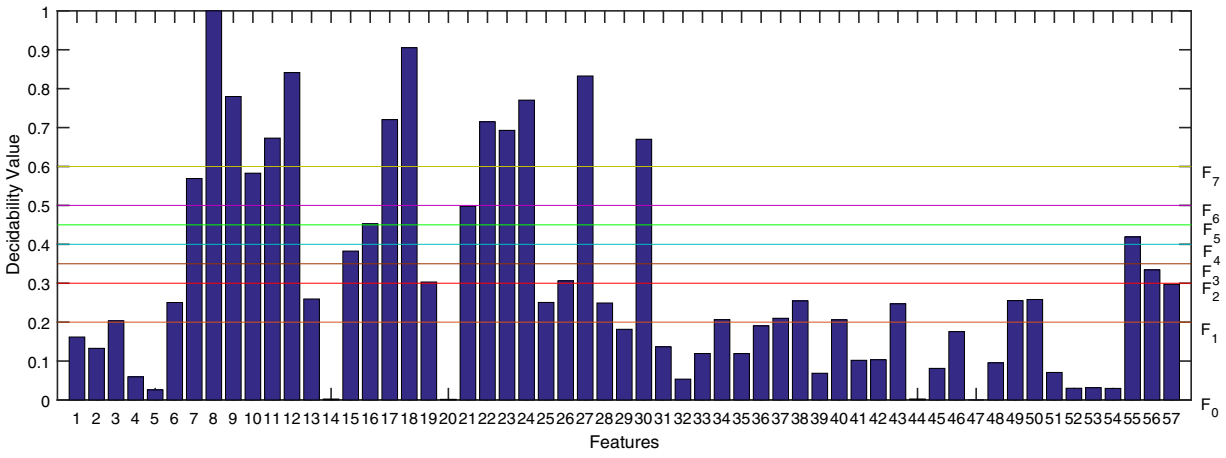

Fig. 3. The barplot of the normalised *Decidability* value per single feature computed according to the formula in (2).

where dec_i is computed by the formula in (2) and the values for τ_j increase with j. It is easy to deduce that $F_{j+1} \subseteq F_j$. In practice, each set of features is contained in the previous one, strictly or not depending on the choice of the thresholds. Fig. 3 shows the thresholds used for the experiments in this paper (see Section 4).

3.3. Feature analysis by Intra-class and Inter-class variability

It is possible to adopt a different measure to describe the discriminative power of the computed features, and to separate "good" features from the bad ones. This entails comparing intra/inter-subject variability characterizing each feature. The underlying assumption is that it is preferable to choose features according to their level of stability within the same subject, as compared with their variability across different subjects. Given a set of hand images $I = I_1, \ldots, I_n$, which belong to a set of gallery subjects $G = G_1, \ldots, G_g$, a first step entails computing an all-against-all distance matrix M_i for each feature f_i, where each element $M_i(l, k)$ is the absolute difference of the measure of f_i computed for I_l and I_k, that is $M_i(l, k) = |f_i(I_l) - f_i(I_k)|$. Let us assume to have a total of s comparisons involving samples belonging to the same subject, and a total of d comparisons involving samples belonging to different subjects. This allows avoiding any assumption on the number of samples per subject, either equal or not for all subjects. We then define:

$$\Delta_{INTRA_i} = \frac{1}{s} \sum_{\substack{I_l, I_k \\ \text{same subjects}}} M_i(l, k) \tag{4}$$

and

$$\Delta_{INTER_i} = \frac{1}{d} \sum_{\substack{I_l, I_k \\ \text{different subjects}}} M_i(l, k) \tag{5}$$

and finally:

$$rank_i = \frac{\Delta_{INTRA_i}}{\Delta_{INTER_i}} \tag{6}$$

Lower values of the rank identify features for which the differences among acquisitions of the same individual have an overall value much lower than those of different individuals. This is a desirable characteristic of a biometric trait. As with *Decidability*, it is possible to group features in subsets F_j of decreasing size according to the condition:

$$F_j = \{f_i : rank_i < \tau_j\} \quad with \quad 0 \leq \tau_j \leq 1 \tag{7}$$

with $rank_i$ for feature f_i computed as in (6) and τ_j increasing with j, that implies $F_j \subseteq F_{j+1}$.

4. Experiments

This section first introduces the characteristics of the dataset used as benchmark for the presented experiments. In the following subsections, three different groups of results will be discussed. The first, in Section 4.2, regards the use of the canonical classes of measures of a hand, namely those related to *Length, Area, Angle* and *Ratio*. These measures refer to the features summarised in Table 1. The following Sections 4.3 and 4.4 deal with the use of the two different metrics introduced in Section 3 (namely the *Decidability* measure and Intra/Inter-class variability ratio) to identify the most representative as well as robust features within the original set.

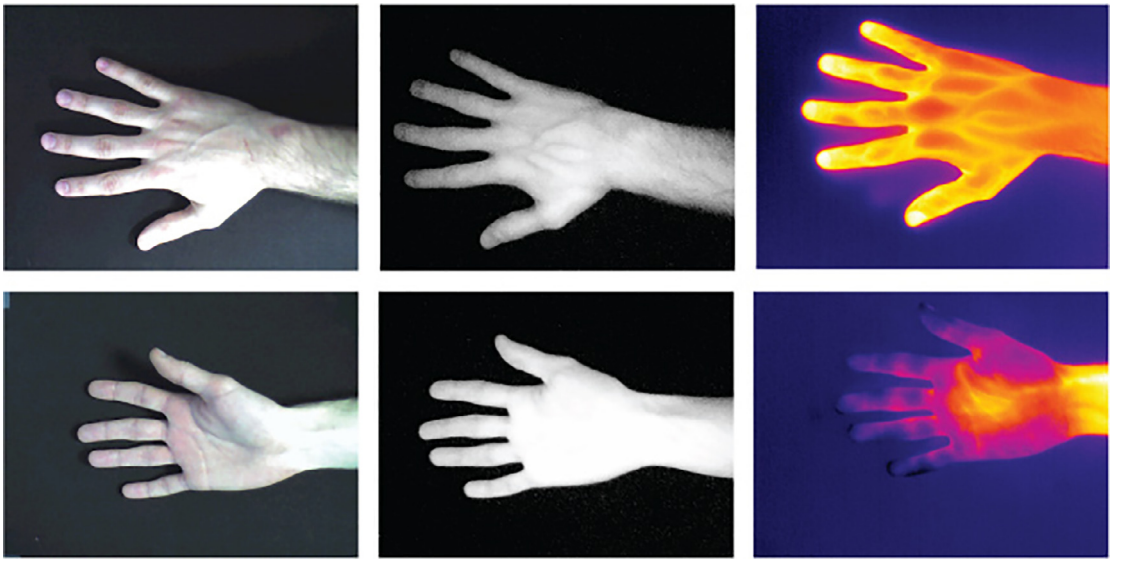

Fig. 4. A sample of the acquisitions from the Technocampus Hand Image Database.

4.1. The dataset used as test-bed

The preliminary experimentation has been carried out using a Samsung Galaxy Note 4 (N910F) equipped with a Sony IMX240 camera. The system acquires frames with a resolution of 800x600. With this setting, the proposed method segments each frame and extracts the considered features in about 250 milliseconds. In the same conditions, the verification time (1:1 matching) is lower than 1 millisecond (precisely about 0.33ms). The user has to hold the mobile device by one hand, and to place the other hand in front of the camera. It would have been possible to design the system so to ask the user to exhibit either the palm or the back of the hand. We chose the second option because the users generally consider this more natural. A minimalist and simple Graphical User Interface (GUI) guides the user during image acquisition. Some preliminary tests were carried out with an in-house dataset captured by the mentioned system. Afterwards, in order to run the experiments presented here, a public dataset was chosen, namely Technocampus Hand Image Database [16,18] (Fig. 4). It includes images of the back of the hand, with characteristics similar to those handled by our system. The reason for choosing such dataset was to allow a fair comparison with other proposals. Actually, most hand datasets used for biometric recognition in literature are rather collected using scanners, or cameras mounted on a support, suitable for the acquisition of images of the palm. Technocampus Hand Image Database is one of the few examples of publicly available datasets collected in the acquisition conditions that match those considered for our system: no pegs or special tips have been used, the areas used for segmentation are correctly filled in all images, and the resolution is compatible with the one we chose. The Technocampus Hand Image Database contains pictures of the right hand of 100 users acquired with a resolution of 640x480 pixels. This resolution is the same achievable by a broad range of cheap mobile devices with limited processing power and low resolution cameras. Each subject has been acquired in five different successive sessions with two acquisitions per session. A session contains images in the visible spectrum, a thermal image and an infrared image, of both back and palm (a sample is shown in Fig. 4). The acquisition device is a thermal commercial camera (Testo 882-3). As mentioned above, the reported experimental results have been obtained using this set of images, which is freely available to researchers.

Another similar dataset is the UST hand dataset [24], which contains hands of 287 subjects acquired in a contactless scenario with an Olympus C-3020 digital camera. No special illumination or pegs have been exploited. However, the resolution of images is 1,280 x 960 pixels, therefore too high to test the performance achievable on most present mobile devices. To the best of our knowledge, it is not possible to find further public datasets with similar features. In fact, quite often, researchers rather use private (and small) datasets like in [22,30,42]. This increases the difficulties of a fair comparison with other state-of-the-art methods, and causes in turn the lack of a broad investigation on hand recognition on mobiles.

Given the above considerations, we compared our proposal with works that meet the following criteria: 1) the acquisition does not involve pegs or constraints; 2) the users place naturally their hands in front of the camera; 3) the users are asked to open their hand so that fingers are clearly separable (this generally substitutes the condition to fill the highlighted areas).

4.2. Canonical features - lengths, angles, areas and ratios

Some of the results presented in this section are from our previous preliminary analysis published in [7]. Being implemented for mobile devices, with limited processing power compared to desktop machines, the Euclidean distance was chosen to match templates in this initial phase since it is simple, not computationally demanding and commonly used in the

Please cite this article as: S. Barra et al., A hand-based biometric system in visible light for mobile environments, Information Sciences (2018), https://doi.org/10.1016/j.ins.2018.01.010

Table 2
The results in terms of EER (Equal Error Rate) for each feature set, namely *Length, Area, Angle* and *Ratio*, whose components are described in Table 1. The ED column shows the results in [7] computed by the Euclidean Distance. The remaining columns stand respectively for BaggedTrees, Fine KNN, Linear Discriminant Analysis, SubSpaceDiscriminant, SubSpace KNN and Weighted KNN. In bold the best classifier for each class of measures. Underlined the best result for each classifier.

Measures	Feat. Set	ED	BT	KNN	LDA	SSD	SKNN	WKNN
Lengths	$f_1, \ldots, f_{30}$	7.2%	1.3%	2.1%	**0.64%**	0.7%	0.8%	1.6%
Areas	$f_{41}, \ldots, f_{51}$	10.6%	4.7%	12.7%	3.8%	4.0%	5.2%	**3.3%**
Angles	$f_{52}, \ldots, f_{57}$	13.1%	10.8%	22.5%	7.9%	**7.3%**	19.9%	8.5%
Ratios	$f_{31}, \ldots, f_{40}$	18.7%	10.1%	20.2%	**3.8%**	5.1%	13.3%	10.5%

Table 3
The results in terms of Recognition Rate obtained by the classifiers over the canonical sets of features. In bold the best classifier for each class of measures

Measures	ED	BT	KNN	LDA	SSD	SKNN	WKNN.
Lengths	85%	88%	97%	**98%**	**98%**	91%	93%
Areas	50%	67%	73%	79%	80%	70%	**81%**
Angles	40%	46%	52%	63%	**65%**	25%	52%
Ratios	42%	62%	62%	**81%**	76%	35%	60%

literature. The main expected outcome from testing the collection of subsets of features obtained by different criteria was to identify the best candidate subset in terms of both robustness and discriminating power. The first experiments considered the collections of features determined by the kind of geometrical measure, as detailed in Table 1, in order to evaluate the discriminating power of each of them. Table 2 summarises the results, in terms of Equal Error Rate (EER), achieved by the four classes used separately, after applying ℓ_1-norm normalisation to the data. The third column, labelled as ED (standardised Euclidean distance), reports the preliminary results achieved in [7]. From those early results, an extended analysis exploited a set of classifiers typically used in machine learning, namely BaggedTrees (BT [29]), Fine KNN, Linear Discriminant Analysis (LDA [11]), SubSpaceDiscriminant (SSD [20]), SubSpace KNN (SKNN [20]) and Weighted KNN (WKNN) (the Classifier Learner app of Matlab Statistics and Machine Learning Toolbox was used [28]). The remaining columns in Table 2 report the EER for these classifiers. As expected, the Euclidean Distance generally achieved the highest EER values (the worse ones). Table 2 shows that all classifiers involved in this study confirmed the reliability of the *Lengths* as features for an accurate recognition. In fact, the lowest equal error rate (EER) is always observed for this normalised class of measures. In other terms, it represents the class that better identifies the users.

However, this comparative study also revealed new insights about the other classes of features, and the possible connections between each other. First of all, most of the classifiers better rated the class of *Ratios* over the class of *Angles*. Secondly, the classifier working on the feature space generated by the LDA was the one that, on average, achieved the best results in terms of EER. Table 3 shows, for the same sets of features, the values achieved for the Recognition Rate (RR). By comparing the results obtained by the classifiers taken into account, LDA again confirmed to be a reasonable good option for evaluating the performance of the proposed approach. It is worth noticing that LDA aims at the same goal of the experiments in this study. It builds a new feature space used to project the original data with the twofold objective of maximising both the discriminating power in the reduced dimensional space, and the separability among classes. Moreover, LDA classifier does not require much processing time to build the model and it returns particularly fast responses, being therefore suited for mobile processing. For these reasons, it represented the best candidate for a thorough evaluation of its benefits compared to the preliminary analysis carried out with Euclidean distance. In the following sections we present the results achieved when trying to reduce the dimension of the feature set, and the increase in performance gained by using LDA afterwards, instead of the Euclidean distance.

4.3. Results by Decidability feature analysis

The results presented above refer to homogeneous sets of features, i.e., sets where all features belong to a same geometrical class. The following goal was to rather identify a combination of possibly heterogeneous features (the best one, and possibly with the lowest cardinality) able to support an accurate recognition of the hands in the dataset. For this reason, a more detailed experimentation aimed at a finer assessment of the robustness of the single measures.

A first set of experiments along this line exploited the results of feature analysis by Decidability metric, according to the procedure presented in Section 3.2.

The described thresholding approach was applied to define eight subsets of features, in order to study the resulting EER curve. The thresholds empirically chosen to build the subsets F_j, $j = 0, \ldots, 8$ are reported in Table 4, with $F_{j+1} \subset F_j$.

Please cite this article as: S. Barra et al., A hand-based biometric system in visible light for mobile environments, Information Sciences (2018), https://doi.org/10.1016/j.ins.2018.01.010

Table 4
The EER of the eight subsets of features identified with (3) by thresholds on the *Decidability* value defined in (2). For each subset, the table columns report the corresponding *Decidability* threshold, the features included and the size of the subset, and the EER achieved by ED and by LDA. The F3 subset, which is mainly built around the computed segments of the hand, minimizes the EER. In bold the best classifier for each subset of features. Underlined the best result for each classifier.

FV	$\tau \geq \ldots$	FEATURES	N.	ED	LDA
F0	0	f_{1-57} (all features)	57	7.9%	**1.14%**
F1	0.2	$f_3, f_6 \ldots f_{13}, f_{15} \ldots f_{19}, f_{21} \ldots f_{28}, f_{30}, f_{34}, f_{37}, f_{38}, f_{40}, f_{43}, f_{49}, f_{50}, f_{55} \ldots f_{57}$	33	6.3%	**1.27%**
F2	0.3	$f_7 \ldots f_{12}, f_{15} \ldots f_{19}, f_{21} \ldots f_{24}, f_{26}, f_{27}, f_{30}, f_{55}, f_{56}$	20	4.2%	**<u>0.9%</u>**
F3	0.35	$f_7 \ldots f_{12}, f_{15} \ldots f_{18}, f_{21} \ldots f_{24}, f_{27}, f_{30}, f_{55}$	17	<u>3.5%</u>	**1.17%**
F4	0.4	$f_7 \ldots f_{12}, f_{16} \ldots f_{18}, f_{21} \ldots f_{24}, f_{27}, f_{30}, f_{55}$	16	3.8%	**1.29%**
F5	0.45	$f_7 \ldots f_{12}, f_{16} \ldots f_{18}, f_{21} \ldots f_{24}, f_{27}, f_{30}$	15	4.1%	**1.18%**
F6	0.5	$f_7 \ldots f_{12}, f_{17}, f_{18}, f_{22} \ldots f_{24}, f_{27}, f_{30}$	13	5.1%	**1.60%**
F7	0.6	$f_8, f_9, f_{11}, f_{12}, f_{17}, f_{18}, f_{22} \ldots f_{24}, f_{27}, f_{30}$	11	5.9%	**1.28%**

Table 4 summarises the results of the thresholding in terms of the produced subsets of features, and of the corresponding achieved EER with Euclidean Distance (ED) and LDA.

By comparing the results obtained with ED and with the LDA classifier, we can observe that the last one significantly reduced the EER even in this group of experiments. The subset that achieved the lowest EER when using the ED measure was *F*3. The subset of features that minimized the EER when using LDA was rather *F*2. Both sets, however, are mainly built from features related to the lengths of the segments of the hand and, interestingly, not all lengths enter the subset *F*3 (included in *F*2 and containing the features with highest *Decidability* values. In order to understand the motivation behind such results, it was useful to carefully observe the acquisitions and the measurements extracted from them. It is worth reminding that the acquisition operation did not involve the usage of any peg, a condition that leaves the user free to put his/her hand in front of the camera as he/she prefers (which is a typical problem of contact-less approaches).

By observing the extracted features in these conditions, it was possible to notice that the point V_1 (i.e. the point that falls within the concavity between thumb and index fingers) was the one detected with lower precision from the segmentation mask. This impacted on the reliability of the measures of all segments where V_1 is one of the endpoints. In turn, the lack of accuracy of this measurement impacted on the others, in the class of ratios and areas, whose computation involves the point V_1 (e.g., the area of the triangle f_{50}, that has a vertex in V_1, which consequently makes f_{40} unreliable). The feature $f55$, which consists of the angle between V_1, V_2 and V_4, represented an exception to this behaviour. Even though it depends on the point V_1, it reported a *Decidability* value above the threshold $\tau = 0.35$ (and 0.4 also) falling inside all subsets *F*2, *F*3 and *F*4. This result is explained by the fact that the angle f_{55} does not exclusively depend on the point V_1, and this makes its *Decidability* still high enough to decrease the EER. As a matter of fact, trying to remove the f_{55} feature from the subset *F*3, an EER of 3.89% was obtained by ED, which was slightly better than leaving this feature, but an EER of 1.18% was obtained by LDA, which was slightly higher than the one achieved maintaining f_{55} in *F*3 (1, 17%); removing the feature also raised the EER to 1.1% in LDA for the subset *F*2.

When dealing with the ED metric, similar issues were observed regarding the measures f_7, f_{13}, f_{19}, which relate to lengths of the index, middle and ring fingers respectively, and their correlated f_{25} and f_{26}. For this collection of features, the problem is the randomness of the inclination of the hand with respect to the camera. It is highly probable that this inclination is different across successive acquisitions of the same user. This condition determines a high component of uncertainty for the measures of the lengths of the fingers. The randomness of the lengths of the fingers in turn propagates errors to the ratio f_{38}. The only feature of this type that achieves a sufficiently high *Decidability* is the length of the index finger (in fact, it is preserved in the *F*3 subset). It is possible to conclude that the index finger is somehow less affected by the randomness of the inclination of the hand during the acquisition, thus effectively contributing to the identification of the user. Passing to results achieved by LDA classifier, the last mentioned issues did not seem to affect its performance: several of the above mentioned lengths appear in the subset *F*2, which achieved a significantly lower EER than the other subsets. Fig. 5 summarises in graphical form the behaviour of the different feature sets with both ED and LDA in terms of EER.

It is worth reminding that, when *Decidability* is used, $F_{j+1} \subset F_j$, so that the sequence of subsets is of decreasing cardinality. As *Decidability* of the single features increases, the sets themselves should provide a decreasing EER. For ED, this was true for sets until *F*3, that actually achieved the best EER with this classifier, but it is possible to notice that after that point the EER started increasing again. This seems to testify that *Decidability* of the single features and their number in a chosen set are complementary factors in reaching the final performance. When the number of features in the used set is too small, the set itself starts losing its classification power. The experiments performed by using LDA produced a less regular trend of the EER curve, that achieved its minimum in the threshold 0.3, that corresponds to the subset *F*2. In any case, the reduction of dimensionality of the input was particularly useful to lower the EER in the experiment with Euclidean distance, thus arriving to a subset consisting of 17 features. On the contrary, LDA needed a slightly higher dimensional space to achieve its best accuracy, which was obtained with the subset *F*2 (20 features). Even though in both experiments most of the lengths were preserved in the best subsets, it can be noticed that the subset *F*2 with LDA (EER = 0.9%) did not outperform the level of performance achieved by using the canonical set of *Lengths* features (which achieved 0.64% of EER, see Table 2). This

Please cite this article as: S. Barra et al., A hand-based biometric system in visible light for mobile environments, Information Sciences (2018), https://doi.org/10.1016/j.ins.2018.01.010

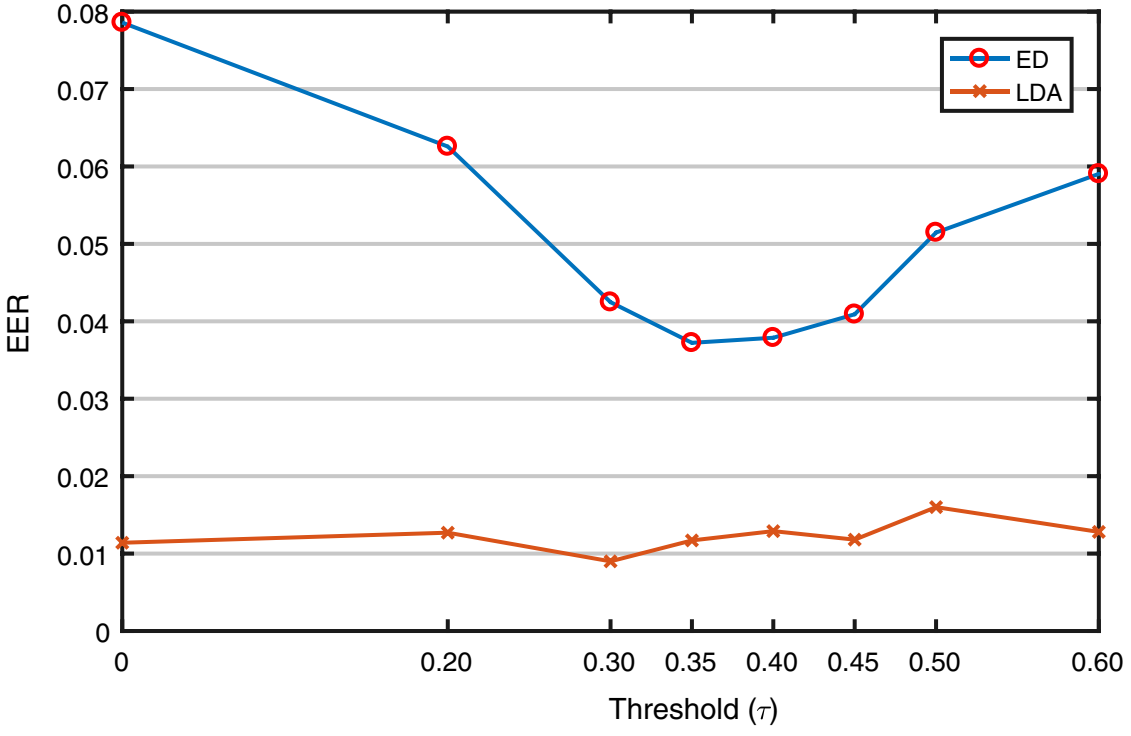

Fig. 5. The behaviour of the EER curves obtained on the subsets of features in Table 4 by using the Euclidean Distance (ED) and the LDA.

Table 5
The EER of the eight subsets of features identified with (7) by thresholds on the *rank* value defined in (6). For each subset, the table columns report the corresponding *rank* threshold, the features included and the size of the subset, and the EER achieved by ED and by LDA. The Euclidean Distance on the F4 subset minimized the EER in [7]. The present results show that LDA achieved better accuracy, with the best EER value obtained on the F5 subset. In bold the best classifier for each subset of features. Underlined the best result for each classifier.

FV	$\cdots \leq \tau$	FEATURES	N.	ED	LDA
F0	0.05	$f_8, f_{13}, f_{19}, f_{25-27}, f_{30}, f_{55}$	8	7.6%	**1.71%**
F1	0.09	$f_8, f_{13}, f_{18-19}, f_{25-28}, f_{30}, f_{55}$	10	6.5%	**1.5%**
F2	0.11	$f_{7-8}, f_{11}, f_{13}, f_{17-19}, f_{22}, f_{25-28}, f_{30}, f_{55}$	14	5.6%	**1.3%**
F3	0.128	$f_{7-8}, f_{11-13}, f_{16-19}, f_{22-23}, f_{25-28}, f_{30}, f_{38}, f_{55}$	17	5.2%	**1.15%**
F4	0.15	$f_{7-8}, f_{11-13}, f_{15-19}, f_{22-30}, f_{37-38}, f_{40}, f_{55}$	23	4.9%	**1.27%**
F5	0.2	$f_{7-13}, f_{15-19}, f_{22-30}, f_{36-38}, f_{40}, f_{50}, f_{55-56}$	28	5.4%	**0.52%**
F6	0.4	$f_{6-13}, f_{15-19}, f_{21-38}, f_{40}, f_{46}, f_{49-51}, f_{55-57}$	39	7.7%	**0.89%**
F7	1	f_{1-57} (all features)	57	7.8%	**1.27%**

result seems to suggest that the reduction of the dimensionality of the input worked better for the Euclidean distance (EER = 7% with the canonical set of *Lengths* features vs. EER = 3.5% with *F*3) than for LDA. On the other hand, the reduced subset *F*2 for LDA experiment allowed to reduce the complexity of the model, while achieving a better result than the complete set of 57 features (EER = 1.14% in Table 4).

4.4. Results by feature analysis based on Intra-class and Inter-class variability

The reduction of the input dimensionality by the *Decidability* metric allowed to reduce the complexity of the model and also allowed to decrease the EER in experiments with both ED and LDA. A further round of experiments dealt with the alternative strategy of comparing Intra/Inter-class variability achieved by single features, according to the analysis described in Section 3.3. Even in this case, the thresholds used to identify subsets of features were chosen empirically, and with those thresholds $F_j \subset F_{j+1}$). When using this criterion, the cardinality of subsets increases with increasing thresholds, since a higher value of the exploited measure identifies less discriminative features. The analysis regarded the effect of τ on the achieved Equal Error Rate (EER) obtained with sets of features according to the rule (7). Table 5 shows the obtained sets of

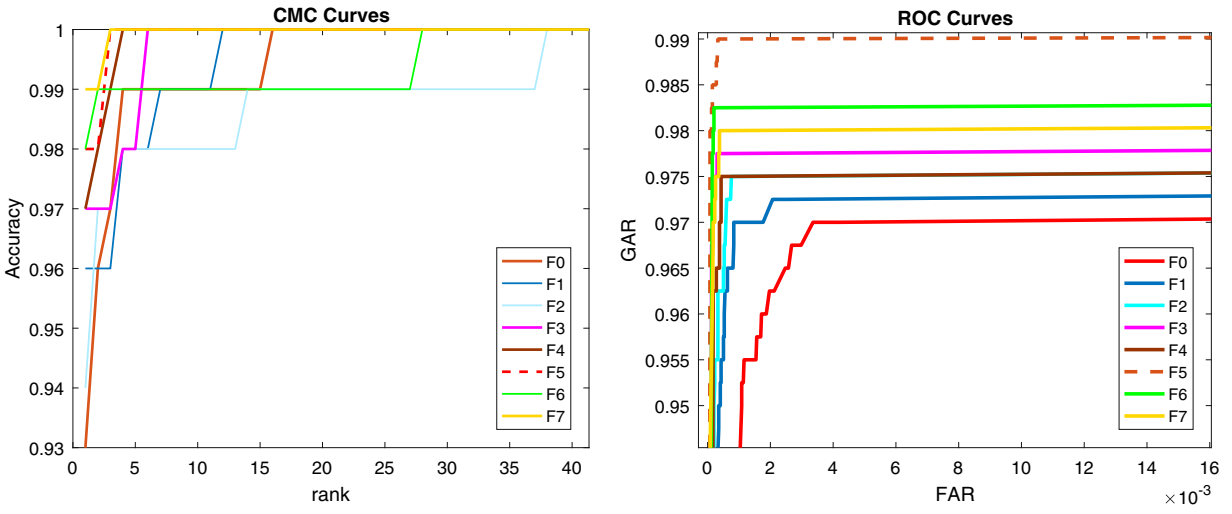

Fig. 6. The level of performance achieved with the subsets in Table 5 when using Intra/Inter-class variability ratio for dimensionality reduction of the input and the LDA classifier on the obtained feature subsets.

features, their size, and the results in terms of EER obtained by Euclidean distance (ED) (related to the preliminary outcomes reported in [7]) and LDA.

The subset achieving the best result using ED was *F*4 (EER = 4.9%) [7], that mainly contains lengths of hand segments, thus further confirming their important role in recognition. However, we can also observe that the best subset exploited by ED did not outperform the best results achieved with the subset *F*3 when using the *Decidability* as a metric for feature analysis and reduction (EER = 3.5% in Table 4). On the contrary, the LDA classifier took advantage from a wider and diversified collection of features (see subsets *F*5 and *F*6) that significantly reduced the EER (0.52% and 0.89% respectively, vs. the best EER = 0.9% in Table 4 obtained with *F*2 identified by *Decidability*). The improvement in performance achieved by LDA was also got with subsets containing most of the lengths measured on hand shape. Fig. 6 shows the CMC (Cumulative Match Curve) and ROC (Receiver Operating Characteristic) curves related to the level of performance achieved with the eight subsets built according to the Intra/Inter-class variability when using LDA for classification, which largely outperforms ED in Table 5. It is interesting to notice that the chosen ranking rule allowed to select a subset of features, in this case the subset *F*5, that achieved an EER of 0.52%, which is the only one even lower than the best result obtained with the canonical subset of *Lengths* (0.64% in Table 2). A further observation regards the composition of *F*5, with respect to the class of *Lengths* in Table 1: while the number of features is much the same (28 vs. 30 out of a complete set of 57), they belong at different extents to different geometric classes (21 *Lengths*, 4 *Ratios*, 1 *Area*, and 2 *Angles*). This result confirmed that it is possible to take advantage from an analysis/selection of features with a twofold benefit: (1) the increase of the level of performance achieved, and (2) a reduction of the input making the computation lighter, which is of paramount importance in mobile computing.

The analysis of the preliminary results obtained in our previous work [7] using the Euclidean Distance as a metric for matching, allowed to suitably reduce the number of features to match and thus the computing demand for mobile devices. The metric of *Decidability* was especially effective in reducing the EER achieved by ED with respect to using the subsets of canonical features as well as using the set of all the features extracted from the hand shape. The best performing subset of features was *F*3 (see Section 4.3) achieving an EER of 3.5%. Considering the simplicity of the approach using the Euclidean Distance and its suitability for mobile computing, the results obtained were considered sufficient for a reliable recognition. However, a deeper analysis of the data carried out exploiting the LDA classifier (chosen among other classifiers typically used in machine learning) revealed a significant improvement in performance while keeping the complexity of the model under control. The impact of such a gaining in performance is rather evident in the plots in Fig. 6. The subset *F*5 achieved an identification accuracy of about 98% (and an EER of 0.52%) by LDA on a selection of 28 features. The crucial aspect to be considered regarding the achieved result is that the reduction of cardinality of the feature set *F*5 lowered the EER over all subsets of canonical features (i.e., *Lengths, Ratios, Angles, Areas*). The aggregated plot in Fig. 7 highlights the margins of improvement of the LDA classifier over the preliminary approach by Euclidean Distance. Among the ROC curves in Fig. 7(a), the curve corresponding to LDA on subset *F*5, selected by Intra/Inter-class variability ratio, and labelled as "LDA intra/inter *F*5" in the plot, shows an extremely peaked curve for the Genuine Acceptance Rate (GAR) at very low values of False Acceptance Rate (FAR). Considering Fig. 7(e), it is also possible to observe the robust separation between genuine and impostors, as compared to all other subsets in both experiments. By comparing LDA experiments only, it is possible to notice that the result on *F*5 (by Intra/Inter-class variability) is more accurate than in the subset *F*2 (by *Decidability*). The close-up in each plot shows the level of separation among genuine and impostors, which is sensibly less accurate in the subsets *F*3 (by Intra/Inter-class variability) and *F*4 (by *Decidability*) processed by the Euclidean Distance.

Please cite this article as: S. Barra et al., A hand-based biometric system in visible light for mobile environments, Information Sciences (2018), https://doi.org/10.1016/j.ins.2018.01.010

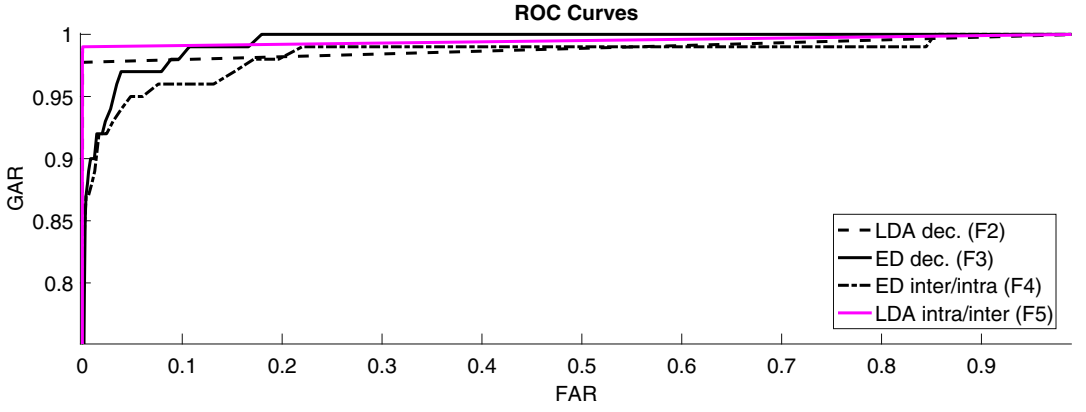

(a) The ROC curves obtained with ED and LDA over the subsets of features that provide the best results (by using both feature analysis techniques - Intra/Inter-class variability and *Decidability*). The x-axis represents the False Acceptance Rate (FAR) while the Genuine Acceptance Rate (GAR) is on the ordinates.

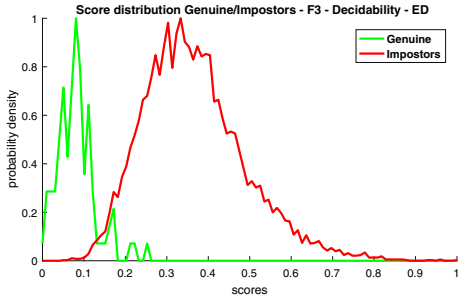

(b) Genuine/Impostor Score Distributions with the subset F3 identified by the *Decidability* ranking (results computed with ED.)

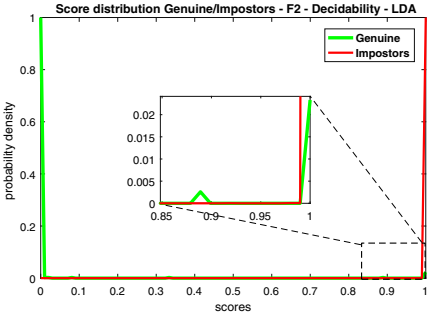

(c) Genuine/Impostor Score Distributions with the subset F2 identified by the *Decidability* ranking (results computed with LDA.)

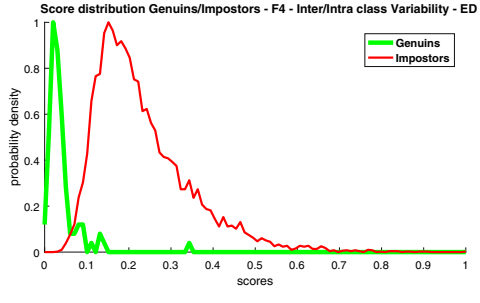

(d) Genuine/Impostor Score Distributions with the subset F4 identified by the Intra/Inter-class variability ratio ranking (results computed with ED.)

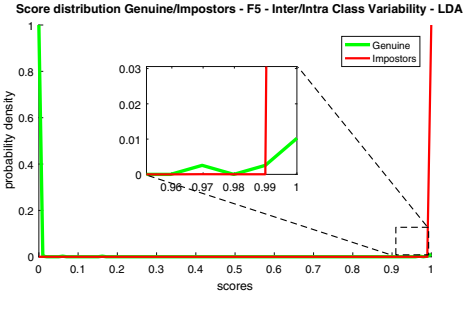

(e) Genuine/Impostor Score Distributions with the subset F5 identified by the Intra/Inter-class variability ratio ranking (results computed with LDA.)

Fig. 7. The overview of the performance achieved with the best selection of features. (a) The ROC curves of the best subset of features; (b,d) the separation between genuine and impostor score distributions by standardised ED using *Decidability* and Intra/Inter-class variability ratio respectively; (c,e) the separation between genuine and impostor score distributions by LDA using *Decidability* and Intra/Inter-class variability ratio respectively.

Please cite this article as: S. Barra et al., A hand-based biometric system in visible light for mobile environments, Information Sciences (2018), https://doi.org/10.1016/j.ins.2018.01.010

Table 6
Literature review on recent works that deal with contact-less biometrics based on hand geometry. (*) When the compared approaches use and combine further features besides those extracted by the hand geometry, the EER reported refers to hand geometry only (when available).

Proposal	Method	Dataset (#Subj.s)	#Feat.s	EER (%)
Sanches et al.[36]	Fusion of features from hand geometry (25 features), palmprint and finger surface.	UST Database (287)	25	3 *
de Santos-Sierra et al.[38]	Recognition based on hand contour.	Proprietary(45)	-	3.7
Kanhangad et al. [22]	Acquisition and combination of 3-D and 2-D features from the hand.	Proprietary (177)	-	6.3 *
Goh Kah Ong et al.[30]	Multi-modal biometric approach which includes hand geometry, palm print, palmar knuckle print, palm vein, and finger vein.	Proprietary (100)	-	3.61
Morales et al.[31]	SVM on features from hand geometry in the visible spectrum.	Proprietary (20)	-	6.3
Luque et al. [26]	Genetic Algorithm+LDA from hand shape geometry	CASIAMS-PalmprintV1 (100) IITD (137)	34	4.64
Sharma et al. [39]	Hand Contour & geometrical features of the hand	IITD (240) Proprietary(50)	121	**0.52 0.31**
do Nascimiento et al [32]	Logist Boot + Random Forest. A combination of 1200 images were used from dorsal and palm acquisitions of hands.	Proprietary (-)	54	-
Kang et al [21]	Fourier descriptors and fingers area functions. Inter-group matching used for dimensionality reduction of the input. Features are extracted from four fingers only (the thumb is ignored).	Hand Geometry DB Part1 (638)	-	3.69
MOHAB [7]	Euclidedan Distance on 17 features extracted by de geometry of the hand.	Technocampus Hand Dataset (100)	17	4.9
This Work (Solution #1)	Features Extraction from hand shape geometry and subset selection with Decidability	Technocampus Hand Dataset (100)	20	**0.9**
This Work (Solution #2)	Features Extraction from hand shape geometry and subset selection with Intra/Inter-Class Variability	Technocampus Hand Dataset (100)	28	**0.52**

The lack of standard tests together with the heterogeneity of datasets (often not publicly available and of different size and nature) makes the comparison with the state-of-the-art a non-trivial task. Several factors affect the achieved performance in each one of the works proposed over recent years, especially for the size of the dataset used and the number of acquisitions per subject. Looking at Table 6, the proposed method ranks well among similar works in literature. Generally, the larger the dataset is, the more reliable and generalizable is the recognition result obtained. Following this observation, the work by Kang et al [21], which used a dataset containing 638 subjects, represents the most accurate result. However, the method proposed therein cannot be considered a valid option for mobile devices, since the acquisitions have been carried out by commercial scanners. It is possible to further observe that the results obtained in our preliminary experimentation using the Euclidean Distance for matching are also comparable with the state-of-the-art. However, the experiments by LDA significantly outperform most of the methods in the literature, thus confirming the competitiveness of the method proposed in this study.

5. Conclusions

This paper has presented a biometric system based on hand geometry, which is suitable to be used on mobile devices. The strength of the proposed approach is that it is oriented to contact-less scenarios, which is a key aspect for mobile devices. Consequently, it does not use any support or driving pegs to help the user to place his/her hand in the desired position during the acquisition. This of course produces images possibly affected by various distortions.

Two different strategies are investigated to analyze the set of features extracted from hand shape, in order to identify the most reliable and robust to distortions.

The results obtained on a public dataset show that the feature extraction and selection strategy is able to achieve a level of performance comparable with the state-of-the-art. Thanks to the low computational demand for human recognition, the proposed method represents a viable solution for devices with low hardware profile and is thus applicable to a wide number of different scenarios, not necessarily limited by the constraints of mobile settings. For example, the analysis of hand features, like shape and geometry as well as texture and finger/palm-print, has significant impact in digital image forensics.

The significant improvement in performance obtained by classifiers typically used in machine learning, suggests that combining alternative sets of features, or computing new ones as well, might even increase the reliability of the proposed method and the related recognition performance. On the other hand, the complexity of the model has to be also taken into account while dealing with the limitation of mobile computing. In this study, the Linear Discriminant Analysis classifier has been chosen for its simple mathematical representation which, consequently, makes its implementation suitable for mobiles. We expect that, by involving new metrics and formal quality measurements of the features, it is still possible to discover alternative sets (the smallest, if possible) of features that can maximise the performances.

Please cite this article as: S. Barra et al., A hand-based biometric system in visible light for mobile environments, Information Sciences (2018), https://doi.org/10.1016/j.ins.2018.01.010

Acknowledgement

This research was partially supported by the Grant PRIN 2015 COSMOS: "COntactlesS Multibiometric mObile System in the wild", Grant number 201548C5NT, funded by the Ministry of Education, University and Research.

References

[1] A.F. Abate, M. Nappi, F. Narducci, S. Ricciardi, Fast iris recognition on smartphone by means of spatial histograms, in: International Workshop on Biometric Authentication, Springer International Publishing, 2014, pp. 66–74.
[2] A.F. Abate, F. Narducci, S. Ricciardi, An image based approach to hand occlusions in mixed reality environments, in: International Conference on Virtual, Augmented and Mixed Reality, Springer, 2014, pp. 319–328.
[3] A.F. Abate, F. Narducci, S. Ricciardi, Biometrics empowered ambient intelligence environment, Atti della Accademia Peloritana dei Pericolanti-Classe di Scienze Fisiche, Matematiche e Naturali 93 (2) (2015) 4.
[4] S. Barra, A. Casanova, M. De Marsico, D. Riccio, Babies: Biometric authentication of newborn identities by means of ear signatures, in: Biometric Measurements and Systems for Security and Medical Applications (BIOMS) Proceedings, 2014 IEEE Workshop on, IEEE, 2014, pp. 1–7.
[5] S. Barra, A. Casanova, F. Narducci, S. Ricciardi, Ubiquitous iris recognition by means of mobile devices, Pattern Recognit. Lett. 57 (2015) 66–73.
[6] S. Barra, M. De Marsico, C. Galdi, W. Harry, FAME: face authentication for mobile encounter, in: IEEE Workshop on Biometric Measurements and Systems for Security and Medical Applications, BioMS 2013, 2013, pp. pp–1.
[7] S. Barra, M. De Marsico, M. Nappi, F. Narducci, D. Riccio, MOHAB: MObile HAnd-based Biometric recognition, in: International Conference on Green, Pervasive, and Cloud Computing, Springer, Cham, 2017, pp. 105–115.
[8] A. Bertillon, Identification anthropométrique: instructions signalétiques, 1, Impr. administrative, 1893.
[9] M. Castrillón-Santana, M. De Marsico, M. Nappi, F. Narducci, H. Proença, Mobile Iris CHallenge Evaluation II: results from the ICPR competition, in: Pattern Recognition (ICPR), 2016 23rd International Conference on, IEEE, 2016, pp. 149–154.
[10] R. Clarke, Human identification in information systems: management challenges and public policy issues, Inf. Technol. People 7 (4) (1994) 6–37.
[11] D.-Q. Dai, P.C. Yuen, Regularized discriminant analysis and its application to face recognition, Pattern Recognit. 36 (3) (2003) 845–847.
[12] M. De Marsico, C. Galdi, M. Nappi, D. Riccio, FIRME: face and iris recognition for mobile engagement, Image Vis. Comput. 32 (12) (2014) 1161–1172.
[13] M. De Marsico, M. Nappi, H. Proença, Results from MICHE II–Mobile Iris CHallenge Evaluation II, Pattern Recognit. Lett. 91 (2017) 3–10.
[14] M. De Marsico, M. Nappi, D. Riccio, H. Wechsler, Mobile Iris CHallenge Evaluation (MICHE)-I, biometric iris dataset and protocols, Pattern Recognit. Lett. 57 (2015) 17–23.
[15] J. Doublet, M. Revenu, O. Lepetit, Robust grayscale distribution estimation for contactless palmprint recognition, in: Biometrics: Theory, Applications, and Systems, 2007. BTAS 2007. First IEEE International Conference on, IEEE, 2007, pp. 1–6.
[16] M. Faundez-Zanuy, J. Mekyska, X. Font-Aragonès, A new hand image database simultaneously acquired in visible, near-infrared and thermal spectrums, Cognit. Comput. 6 (2) (2014) 230–240.
[17] M.A. Ferrer, F. Vargas, A. Morales, Bispectral contactless hand based biometric system, in: Telecommunications (CONATEL), 2011 2nd National Conference on, IEEE, 2011, pp. 1–6.
[18] X. Font Aragonés, M. Faúndez Zanuy, J. Mekyska, Thermal hand image segmentation for biometric recognition, IEEE Aerospace Electron. Syst. Mag. 28 (6) (2013) 4–14.
[19] Y. Han, T. Tan, Z. Sun, Y. Hao, Embedded palmprint recognition system on mobile devices, in: International Conference on Biometrics, Springer, 2007, pp. 1184–1193.
[20] T.K. Ho, The random subspace method for constructing decision forests, IEEE Trans. Pattern Anal. Mach. Intell. 20 (8) (1998) 832–844.
[21] W. Kang, Q. Wu, Pose-invariant hand shape recognition based on finger geometry, IEEE Trans. Syst. Man Cybern. Syst. 44 (11) (2014) 1510–1521.
[22] V. Kanhangad, A. Kumar, D. Zhang, A unified framework for contactless hand verification, IEEE Trans. Inf. Forensics Secur. 6 (3) (2011) 1014–1027.
[23] A. Kong, D. Zhang, M. Kamel, A survey of palmprint recognition, Pattern Recognit. 42 (7) (2009) 1408–1418.
[24] A. Kumar, D.C. Wong, H.C. Shen, A.K. Jain, Personal verification using palmprint and hand geometry biometric, in: International Conference on Audio-and Video-Based Biometric Person Authentication, Springer, 2003, pp. 668–678.
[25] Y. Luo, S.C. Sen-ching, R. Lazzeretti, T. Pignata, M. Barni, Anonymous subject identification and privacy information management in video surveillance, Int. J. Inf. Secur. (2017) 1–18.
[26] R.M. Luque-Baena, D. Elizondo, E. López-Rubio, E.J. Palomo, T. Watson, Assessment of geometric features for individual identification and verification in biometric hand systems, Expert Syst. Appl. 40 (9) (2013) 3580–3594.
[27] M. Maguire, The birth of biometric security, Anthropol. Today 25 (2) (2009) 9–14, doi:10.1111/j.1467-8322.2009.00654.x.
[28] MathWorks, Train classification models in classification learner app, 2015, (https://www.it.mathworks.com/help/stats/train-classification-models-in-classification-learner-app.html). [Online; accessed 19-July-2017].
[29] N. Meinshausen, Quantile regression forests, J. Mach. Learn. Res. 7 (Jun) (2006) 983–999.
[30] G.K.O. Michael, T. Connie, A.B.J. Teoh, A contactless biometric system using multiple hand features, J. Visual Commun. Image Represent. 23 (7) (2012) 1068–1084.
[31] A. Morales, M.A. Ferrer, J.B. Alonso, C.M. Travieso, Comparing infrared and visible illumination for contactless hand based biometric scheme, in: 2008 42nd Annual IEEE International Carnahan Conference on Security Technology, IEEE, 2008, pp. 191–197.
[32] M.V. do Nascimento, L.V. Batista, N. Cavalcanti Jr, A new approach to biometric recognition based on hand geometry, in: Proceedings of the 30th Annual ACM Symposium on Applied Computing, ACM, 2015, pp. 59–65.
[33] J. Neves, F. Narducci, S. Barra, H. Proença, Biometric recognition in surveillance scenarios: a survey, Artif. Intell. Rev. 46 (4) (2016) 515–541.
[34] H. Proenca, J.C. Neves, S. Barra, T. Marques, J.C. Moreno, Joint head pose/soft label estimation for human recognition in-the-wild, IEEE Trans. Pattern Anal. Mach. Intell. 38 (12) (2016) 2444–2456.
[35] A. Ross, A. Jain, A prototype hand geometry based verification system, in: Proceedings of 2nd Conference on Audio and Video Based Biometric Person Authentication, 1999, pp. 166–171.
[36] T. Sanches, J. Antunes, P.L. Correia, A single sensor hand biometric multimodal system, in: Signal Processing Conference, 2007 15th European, IEEE, 2007, pp. 30–34.
[37] R. Sanchez-Reillo, C. Sanchez-Avila, A. Gonzalez-Marcos, Biometric identification through hand geometry measurements, IEEE Trans. Pattern Anal. Mach. Intell. 22 (10) (2000) 1168–1171.
[38] A. de Santos-Sierra, C. Sánchez-Avila, G.B. del Pozo, J. Guerra-Casanova, Unconstrained and contactless hand geometry biometrics, Sensors 11 (11) (2011) 10143–10164.
[39] S. Sharma, S.R. Dubey, S.K. Singh, R. Saxena, R.K. Singh, Identity verification using shape and geometry of human hands, Expert Syst. Appl. 42 (2) (2015) 821–832.
[40] P. SociaLab, Nice:ii evaluation, 2010, (http://nice2.di.ubi.pt/evaluation.htm). [Online; accessed 20-July-2017].
[41] P. Varchol, D. Levicky, Using of hand geometry in biometric security systems, Radioengineering-Prague- 16 (4) (2007) 82.
[42] A.L. Wong, P. Shi, Peg-free hand geometry recognition using hierarchical geometry and shape matching., in: MVA - IAPR Workshop on Machine Vision and Applications, Citeseer, 2002, pp. 281–284.
[43] M. Wong, D. Zhang, W.-K. Kong, G. Lu, Real-time palmprint acquisition system design, IEE Proc.-Vision Image Signal Process. 152 (5) (2005) 527–534.

Please cite this article as: S. Barra et al., A hand-based biometric system in visible light for mobile environments, Information Sciences (2018), https://doi.org/10.1016/j.ins.2018.01.010